



# Catalytic activity of unsupported Pd-Pt nanoalloys with low Pt content towards formic acid oxidation

Barbara Gralec, Adam Lewera\*

University of Warsaw, Department of Chemistry, Biological and Chemical Research Centre, ul. Żwirki i Wigury 101, 02-089 Warsaw, Poland

## ARTICLE INFO

### Article history:

Received 17 December 2015  
Received in revised form 7 March 2016  
Accepted 30 March 2016  
Available online 31 March 2016

### Keywords:

Formic acid oxidation  
Electrocatalysis  
Platinum  
Palladium

## ABSTRACT

We present the results of systematic investigation of catalytic activity of unsupported Pd-Pt nanoparticles towards formic acid oxidation. Investigation of unsupported nanoparticles allowed us to address the changes in catalytic activity caused by interactions between Pt and Pd and to exclude the possible influence of the support. While full range of Pt concentration in Pd was covered, we focused on the role of small amounts of Pt on the catalytic activity of Pd nanoparticles. We determined that formic acid oxidation half-wave potential was lower on Pd-Pt nanoparticles containing small amounts of Pt as compared to pure Pd nanoparticles. In comparison to pure Pd, Pd-Pt nanoparticles also exhibited higher formic acid electrooxidation current density observed in cathodic scans during voltammetric experiments. We attribute the changes in the half-wave potential mostly to the changes of surface electronic properties due to interactions between Pt and Pd, and the changes in catalytic current density to interplay between modified electronic properties and changes in surface morphology.

© 2016 Elsevier B.V. All rights reserved.

## 1. Introduction

Formic acid oxidation reaction on noble metals has been extensively studied in the past [1–5] and is still under investigation due to its importance to low-temperature direct formic acid fuel cells (DFAFC) [6–9]. Additionally formic acid oxidation, due to its simplicity, is a model reaction to study the relationship between surface properties and catalytic activity [10–12].

Among the noble metals platinum and palladium are most often used as catalysts of formic acid electrooxidation. On Pt, Pd and Pd-Pt alloys this reaction follows a so-called “dual pathway” mechanism, namely formic acid can undergo dehydrogenation leading directly to CO<sub>2</sub> (not involving strongly adsorbed CO, CO<sub>ads</sub>, as an intermediate) or dehydration leading to formation of CO<sub>ads</sub> and its possible further oxidation to CO<sub>2</sub> [1,2]. Direct path (dehydrogenation) is operative at relatively low potentials but, in case of Pt, strongly adsorbed CO<sub>ads</sub> quickly blocks the surface sites, causing overall low activity of Pt in formic acid oxidation at low potentials [13]. On the contrary for Pd the poisoning by CO<sub>ads</sub> at low potentials is much slower [9,14–16] and the direct path (dehydrogenation) is operative to a much large extend [7]. As a result Pd is significantly more active than Pt towards formic acid oxidation at low potential [7].

It is however still unclear how the catalytic activity of Pd-Pt alloys towards formic acid scale with composition. There have been reports claiming that Pd-Pt alloys exhibit higher catalytic activity towards formic acid oxidation than pure Pd [17,18], where other authors found otherwise [19]. This subject is especially important, as alloying, except obvious change in surface composition, can lead to material with modified electronic properties [20–25], which can potentially be responsible for the synergistic effect of both metals on formic acid oxidation. More insight into this phenomenon would help to better understand the relationship between catalytic and electronic properties.

To pinpoint the possible changes of catalytic activity caused by changes in electronic structure, investigation of unsupported Pd-Pt nanoparticles is especially important, as the support may also play a significant role in modifying the electronic and catalytic properties of the material [26–31]. In practice various supporting materials are used—from mostly inert carbon nanoparticles (such as Vulcan XC-72), ordered carbonaceous materials [30,31] to metal oxides, which are known to (beneficially) modify the catalytic properties of the deposited metals via a so-called Strong Metal-Support Interactions (SMSI) [32–35]. However the unsupported catalysts allow for better understanding of the role of other factors influencing the catalytic activity, which can be otherwise masked by a large influence of the support on the catalytic activity. In this context the investigation of unsupported Pd-Pt nanoparticles provided here can help in gaining more knowledge on the catalytic processes, especially

\* Corresponding author.

E-mail address: [alewera@chem.uw.edu.pl](mailto:alewera@chem.uw.edu.pl) (A. Lewera).

taking into account the fact that the reports on formic acid activity of unsupported Pd-Pt nanoparticles are scarce [36–38] and limited to a narrow range of relatively high Pt concentration. We focused here on Pd-Pt nanoalloys with relatively low Pt amount to pinpoint the subtle changes in activity caused by changes in surface morphology and the possible resulting electronic effects when Pt is incorporated into Pd. To our knowledge no reports on formic acid oxidation on unsupported Pd-Pt nanoparticles with low Pt content exists.

## 2. Experimental

All chemicals used were of analytical grade and were used without further purification. For electrochemical experiments sulfuric(VI) acid (p.a., 95–97%, POCh, Gliwice, Poland) and formic acid (p.a., 98–100%, POCh, Gliwice, Poland) were used. All solutions were prepared using deionized (Millipore Milli-Q) water. N6.7 Argon (BIP plus, Air Products) was used to de-aerate the solutions for electrochemical experiments.

Unsupported ultra-pure Pd-Pt nanoparticles were synthesized without the use of any surfactant, using modified polyol method as described by us before [39]. In short, to obtain Pd-Pt nanoparticles with desired Pd to Pt molar ratio in the resulting nanoparticles,  $\text{PdCl}_2$  (p.a., POCh, Gliwice, Poland) and  $\text{K}_2\text{PtCl}_4$  (99.9%, Alfa Aesar) were used. The amounts of both precursors were pre-weighed to obtain both the desired Pt:Pd molar ratio and the total amount of metals equal to 0.5 mmol. Pre-weighed precursors were added to 110 mL of Ethylene Glycol (analytical grade, 99.5%, Fluka) at room temperature, followed by heating at  $5^\circ\text{C min}^{-1}$  ratio until  $110^\circ\text{C}$ , then kept for 5 min and left to cool.

For the electrochemical characterization of Pd-Pt nanoparticles CH Instruments Model 660 potentiostat was used. All electrochemical measurements were performed in three-electrode configuration. The reference electrode was  $\text{Hg}|\text{Hg}_2\text{SO}_4|0.5\text{M H}_2\text{SO}_4$  electrode (double bridged with 0.5 M  $\text{H}_2\text{SO}_4$  in the salt bridge), and a gold foil of large area (a few  $\text{cm}^2$ ) pre-cleaned in piranha solution was used as the counter electrode. Potential of the reference electrode was periodically checked against a reversible hydrogen electrode (RHE); and all potentials have been recalculated and expressed versus the RHE. Active surface area was determined based on surface oxygen reduction charge, assuming  $420 \mu\text{C cm}^{-2}$ .

The working electrode consisted of gold substrate,  $\varnothing 2\text{ mm}$  (BASi, USA), which was polished before each experiment using polishing cloths containing diamond suspensions, with decreasing diamond size (6, 1, and  $0.05 \mu\text{m}$ ). Onto the polished gold substrate, the aqueous suspension ( $0.5 \mu\text{L}$ ) of the investigated nanoparticles was deposited and left to dry without use of any binding agent, as described elsewhere [40].

## 3. Results and discussion

Morphology of the unsupported Pd-Pt nanoparticles obtained using the same method as used here has been extensively investigated by us before [41]. However due to small differences in physicochemical parameters of precursor reduction (lower temperature and shorter reduction time) we repeated the most critical experiments and the discussion of the results is presented below.

The TEM images of the investigated nanoparticles are presented in Fig. S1 (Supplementary information) and average sizes are given in Table TS1 (Supplementary information). In short the mean size of the investigated nanoparticles is between 8 and 20 nm for Pd-Pt nanoalloys, where pure Pt nanoparticles are slightly smaller (5 nm) and pure Pd nanoparticles slightly larger (32 nm). Those results are very similar to what we obtained previously [41]. It is worth noting that the nanoparticles were synthesized in absence of any

**Table 1**

CO stripping charge ( $Q_{\text{CO}}$ ) to charge of surface oxide reduction ( $Q_{\text{oxides}}$ ) for all investigated samples.

Sample (Pd-Pt ratio)	100:0 (Pt)	50:50	20:80	10:90	5:95	2:98	1:99	0:100 (Pd)
$Q_{\text{CO}}/Q_{\text{oxides}}$	0.99	0.97	0.83	0.84	0.83	0.83	0.84	0.84

surfactant, which caused the observed increase of the size of the resulting nanoparticles and the overall wider distribution of nanoparticles' size (Fig. S1). However the lack of surfactant has a significant advantage, because the nanoparticles obtained in its absence did not required any cleaning steps [39]. Ultra-high surface purity of the nanoparticles obtained also eliminates the need for the pre-cleaning of the nanoparticles, as commonly made, i.e. using potential cycling. Cleaning Pd-Pt nanoparticles using potential cycling leads to subsequent surface oxidation-reduction, which could alter the morphology of the material, for instance via cathodic dissolution of less noble Pd. Ultra high purity of our nanoparticles was confirmed by electrochemical data, presented in Fig. 1, which were collected for as-synthesized Pd-Pt nanoparticles.

The overall nanoparticle composition as determined by ICPMS is in good agreement (within 1%) with the amount of precursor used, thus we refer to the samples investigated using nominal composition. Composition data for all nanoparticles is presented in Supplementary information (Table TS3).

To discuss the possible deviations from homogeneity for Pd-Pt nanoalloys we will refer to our previous extensive study of morphology of unsupported Pd-Pt nanoalloys [41]. Namely X-ray diffraction (XRD) experiments for identical Pd-Pt nanoparticles led to linear dependence of lattice parameter with composition, which suggest an ideal homogeneous alloying, but as it was discussed in Ref. [41] it can be misleading and in fact significant inhomogeneities can be undetected in XRD experiments for nanoparticles [42]. Based on previous study using XPS, ICPMS, XRD and hydrogen adsorption we determined that segregation of Pt to surface of unsupported Pd-Pt nanoparticles occur [42], which is in agreement with studies of thin Pd-Pt films [18].

To determine the electrochemically active surface area (ECSA) we decided on using the surface oxides reduction peak, instead of oxidation of adsorbed CO ("CO stripping") due to literature reports showing that even at full coverage of CO adsorbed on Pd, mixed linear and bridge bonded CO exists [43–45]. The charge of oxidizing a linearly adsorbed CO is  $420 \mu\text{C cm}^{-2}$ , where charge of oxidation of bridge bonded CO is  $210 \mu\text{C cm}^{-2}$ . As a result the charge associated with CO stripping on Pd-Pt alloys cannot be reliably correlated to ECSA as the amounts of linearly and bridge bonded CO are unknown, and vary with composition. Generally it was found that on pure Pd between 50 and 70% of CO is bonded linearly (see Ref. [45] and references therein). On the contrary the surface oxide reduction charge for Pd ( $424 \mu\text{C cm}^{-2}$  [46]), is virtually identical to Pt surface oxide reduction ( $420 \mu\text{C cm}^{-2}$ ), resulting in more dependable ECSA determination for Pd-Pt alloys, regardless of composition. To check that assumption for each sample we performed CO stripping experiment, directly followed by surface oxides reduction experiments. The fractions of charge of CO stripping ( $Q_{\text{CO}}$ ) to charge of surface oxide reduction ( $Q_{\text{oxides}}$ ) are presented in Table 1, where the raw data are presented in Table TS2 (Supplementary information).

The data presented in Table 1 shows that the CO stripping charge, relative to surface reduction charge is almost identical for Pt and Pt-rich sample, where for other samples CO stripping charge is lower than surface oxide reduction charge, which is in agreement with the possible presence of bridge bonded CO on Pd. It is also interesting to note that for Pt:Pd 50:50 the CO and surface oxide reduction charge also match, which suggests Pt surface segregation in case of the investigated nanoparticles.

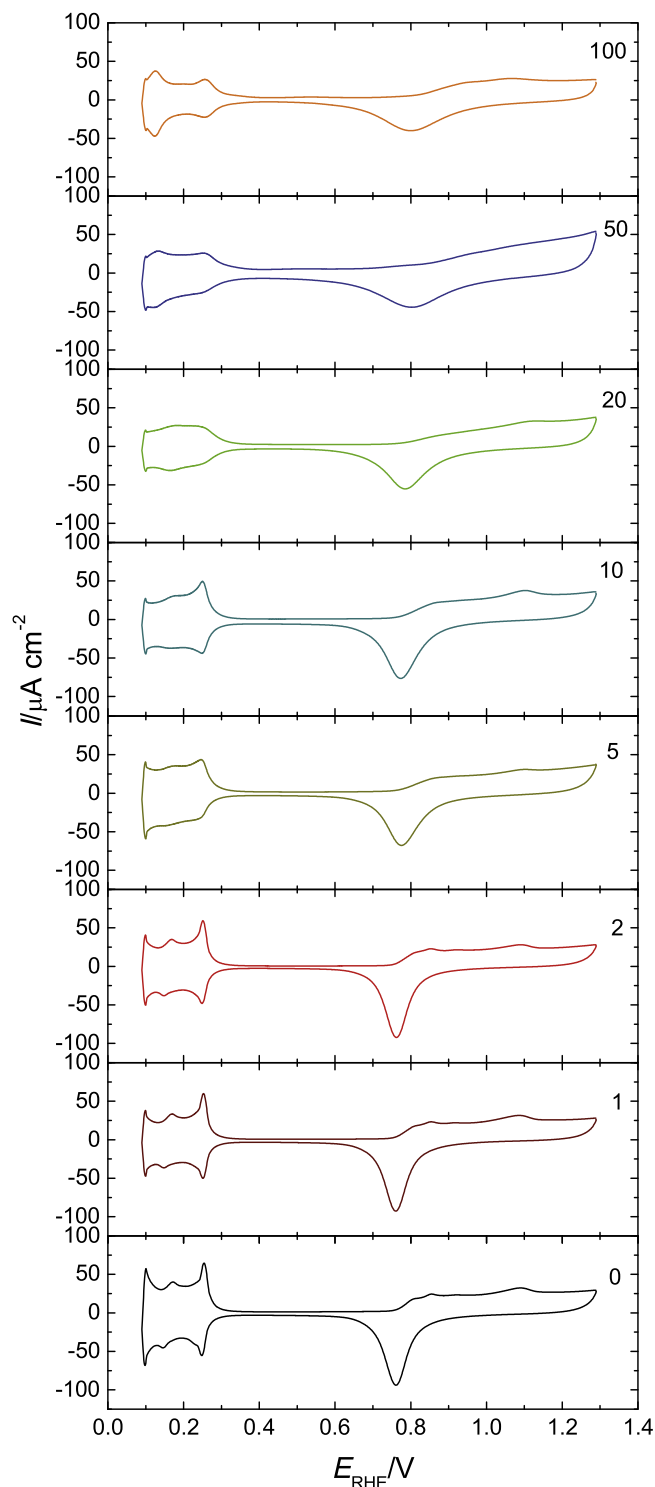


**Fig. 1.** Voltammetric characterization of Pd-Pt nanoalloys in 0.5 M  $\text{H}_2\text{SO}_4$ .  $v = 20 \text{ mV s}^{-1}$ . Numbers denote Pt content in atomic %. Colors were used consistently for all figures to denote the Pt concentration in the investigated nanoparticles.

Voltammetric characterization of Pd-Pt nanoparticles is presented in Fig. 1.

As it can be observed voltammograms registered for Pd-Pt nanoparticles exhibit two distinct regions: hydrogen adsorption-desorption below 300 mV and surface oxidation/surface reduction at potentials above 600 mV. The changes in CV shape, related to changes in composition, can be observed for both regions. In particular surface reduction peak potential changes from 760 mV

for pure Pd to 800 mV for pure Pt (Fig. 1). It is interesting to note that virtually identical potentials of surface oxide reduction can be observed for Pt and Pd-Pt 50:50. This is another suggestion for Pt surface segregation in Pd-Pt nanoparticles (as suggested by CO stripping charge to surface oxide reduction charge, Table 1 above). It can be also observed that the hydrogen region evolves from the signature typical for pure Pd to those of pure Pt when Pt amount increase, with a featureless hydrogen adsorption/desorption region for nanoparticles containing 20 at.% of Pt (cf. Fig. 1 in the 0–300 mV region).

Formic acid oxidation experiments were performed on Pd-Pt nanoparticles in 0.5 M  $\text{HCOOH}$  in 0.5 M  $\text{H}_2\text{SO}_4$ . Relatively high concentration of both, formic acid and the supporting electrolyte was used to avoid current oscillations, which are sometimes observed for formic acid oxidation on Pd in the cathodic scan for low  $\text{HCOOH}$  concentration [47]. From our experience current oscillations sometimes occurred even for 0.5 M  $\text{HCOOH}$  in 0.5 M  $\text{H}_2\text{SO}_4$ . When oscillations were observed the amount of nanoparticles deposited on electrode substrate was decreased and experiment was repeated. For clarity the anodic and cathodic scans are presented on separate figures (Fig. 2A and B).

In the anodic scan two regions changed as a function of Pt concentration: i) the first anodic peak at ca. 350 mV quickly decreased as Pt concentration increased; and ii) small peak at ca. 900 mV increased when Pt concentration increased. Additionally for pure Pd the peak at ca. 350 mV is not well separated and can be seen as inflection point at ca. 320 mV on the CV curve, followed by second peak at ca. 500 mV. Interestingly that second peak was not observed on any other sample, but a similar shape of CV for formic acid oxidation, including the inflection point can be also observed in the data available in the literature (i.e. cf. Fig. 5a in Ref. [17]).

Above mentioned signals can be attributed to the following processes: anodic peak at 350 mV is associated with oxidation of formic acid to  $\text{CO}_2$  in the direct path (i.e. not involving the  $\text{CO}_{\text{ads}}$ ) where the peak at 900 mV is the oxidative stripping of adsorbed CO followed by oxidation of  $\text{HCOOH}$  on freshly released surface sites [48], which allows for oxidation of formic acid via indirect mechanism. This process stops when surface oxides are formed (see Fig. 2A).

As it can be seen for unsupported Pd-Pt nanoparticles (Fig. 2) the direct path of formic acid oxidation is operative only on Pd-rich nanoparticles (80% Pd or more); for nanoparticles containing not more than 2 at.% of Pt it is the dominant process, and it can be observed, albeit to a much lower degree, on nanoparticles containing up to 80 at.% of Pd. For nanoparticles containing less than 80 at.% of Pd the catalytic currents in low potential region were virtually non-existent. To better illustrate the evolution of voltammograms as a function of composition, and to investigate the possible reasons for decrease of catalytic currents as small amounts of Pt are introduced into Pd matrix, CVs for Pd-Pt containing 5 at.% or less of Pt, and those for samples containing more than 5 at.% were plotted in separate figures (Figs. 3 and 4 respectively).

It can be observed that the CO stripping peak (Figs. 3 and 4, at ca. 900 mV in the anodic scan) is present only for nanoparticles containing at least 5 at.% of Pt. This suggests that the surface of other nanoparticles (containing less than 5 at.% of Pt) within the time limit of the experiment is not significantly poisoned by strongly adsorbed CO. This aspect requires short discussion, as the accumulation of CO during formic acid oxidation at low potential is the subject of a debate. Since the first experiments regarding this formic acid oxidation on Pd it was assumed, based on IRAS or ATR-SEIRAS spectroscopic studies, that at low potentials no adsorbed CO exists [14,49,50]. However more recent research using more sensitive ATR-SEIRAS set-up pointed out that slow accumulation of CO on Pd during low potential oxidation of more concentrated formic acid solution is possible [15,16,51]. The reason why we do not observe adsorbed CO on samples containing less than 5 at.%

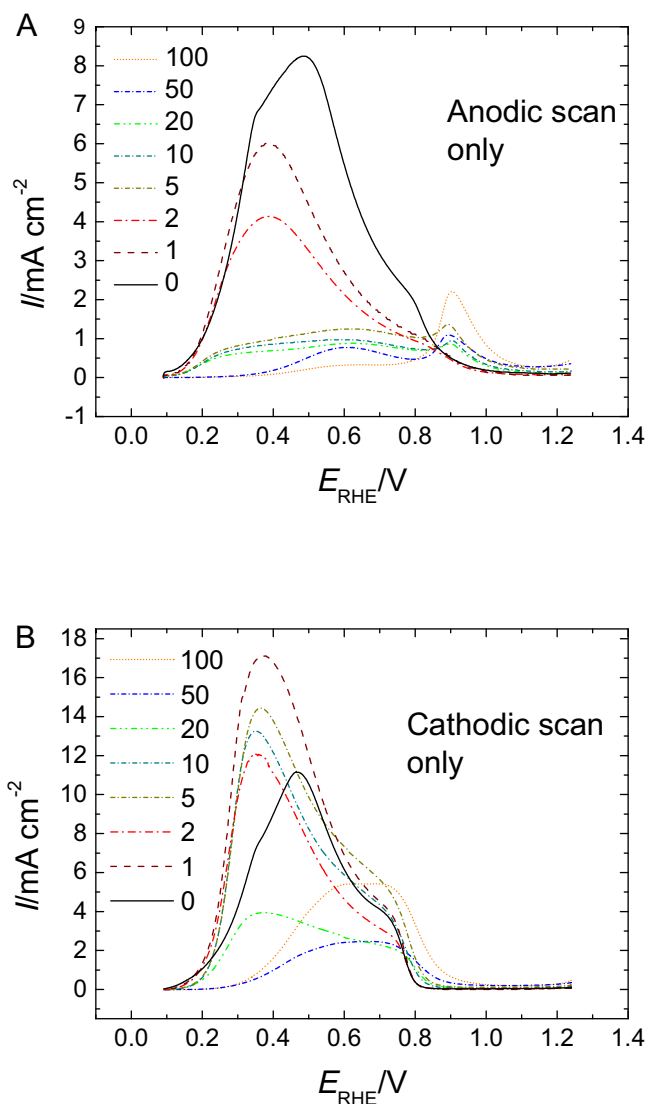


**Fig. 2.** Electrochemical oxidation of formic acid on Pd-Pt nanoparticles investigated using cyclic voltammetry. 0.5 M HCOOH + 0.5 M H<sub>2</sub>SO<sub>4</sub>,  $\nu = 20 \text{ mV s}^{-1}$ . For clarity anodic and cathodic scans were presented on separate figures (A and B, respectively). Numbers in the legend denote Pt content in atomic percents.

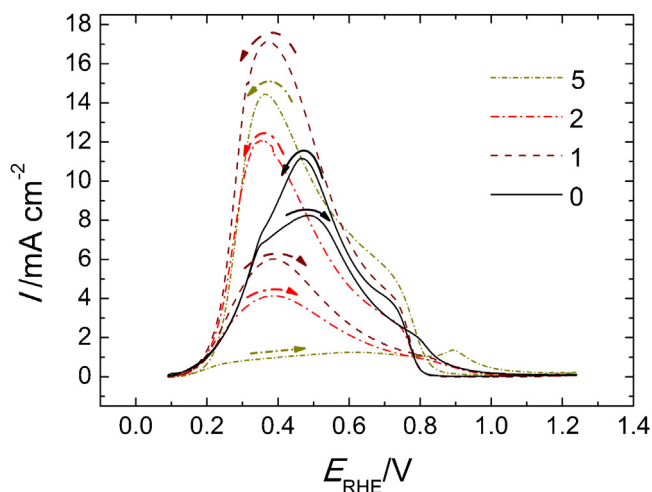


**Fig. 3.** Electrochemical oxidation of formic acid on Pd-Pt nanoparticles with low Pt content, investigated using cyclic voltammetry. 0.5 M HCOOH + 0.5 M H<sub>2</sub>SO<sub>4</sub>,  $\nu = 20 \text{ mV s}^{-1}$ . Arrows show the direction of potential change. Numbers in the legend denote Pt content in atomic percents.

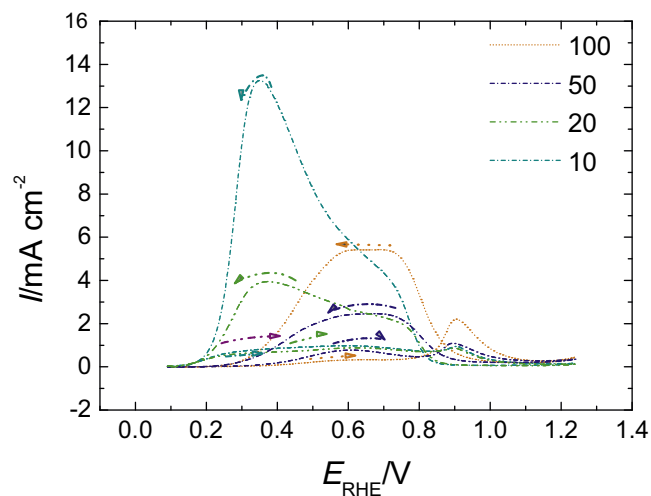


**Fig. 4.** Electrochemical oxidation of formic acid on Pd-Pt nanoparticles containing 10 or more at.% of Pt, investigated using cyclic voltammetry. 0.5 M HCOOH + 0.5 M H<sub>2</sub>SO<sub>4</sub>,  $\nu = 20 \text{ mV s}^{-1}$ . Arrows show the direction of potential change. Numbers in the legend denote Pt content in atomic percents.

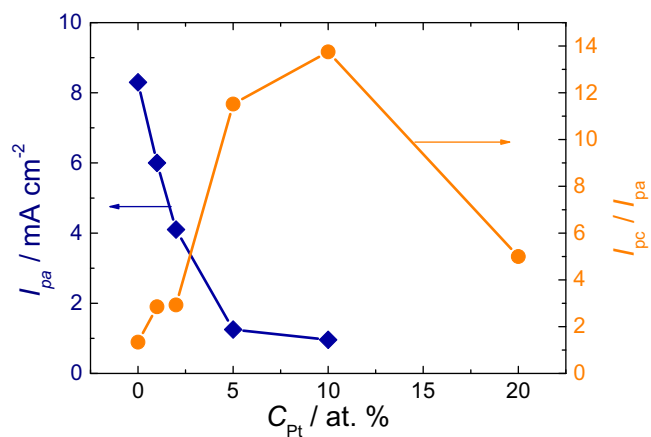


**Fig. 5.** Peak current density of formic acid oxidation at potential lower than 400 mV in the anodic scan ( $I_{pa}$ ) (left blue axis, data points marked by rotated squares) and the relative formic acid oxidation peak current density in the cathodic scan ( $I_{pc}$ ) to the formic acid oxidation peak current density in the anodic scan ( $I_{pa}$ ) (right orange axis, data points marked as circles) as a function of Pt content in Pd-Pt nanoparticles.

(Fig. 3) is most probably the relatively short time frame of the experiment and lower concentration of formic acid used by us as compared to experiments, where it was observed [15,16,51].

The observation of strong influence of small amounts of Pt (1–20 at.%) on current density related to catalytic electrooxidation of formic acid on Pd-Pt nanoparticles should be first explained based on the changes in surface composition and the possible role of small amounts of Pt incorporated into Pd on formic acid oxidation mechanism on the resulting surface. To better illustrate the discussed relations, the peak current density of formic acid oxidation at potential lower than 400 mV in the anodic scan ( $I_{pa}$ —as seen in Fig. 2A) and the relative formic acid oxidation peak current density in the cathodic scan ( $I_{pc}$ —as seen in Fig. 2B) to  $I_{pa}$  were plotted as a function of Pt content in Pd-Pt nanoparticles (Fig. 5). It can be observed that  $I_{pa}$  decreased monotonically as Pt content increased, where  $I_{pc}$  to  $I_{pa}$  showed a volcano-type behavior with maximum at 10 at.% of Pt. We explain those observations considering how alloying of Pt with Pd influences the number of adjacent Pd sites required to adsorb formic acid molecule, the role of isolated Pt atoms on Pd-Pt surface, the role of Pt surface segregation and the

possible changes in surface electronic properties when Pt is alloyed with Pd.

It is postulated that on VIII B group transition metal adsorbed formate occupy either one (monodentate or bidentate configuration) or two (bridge configuration) adjacent metal sites, and on Pt the bridge configuration dominates, however on Pd the formate adsorption configuration is under debate [52]. Regardless of the exact adsorption configuration, obviously the number of multiple adjacent Pd sites will decrease more rapidly than linearly as a function of decreasing Pd amount, potentially causing the decrease of catalytic current. At the same time however low amounts of Pt in Pd-Pt alloys can have a promoting effect on catalytic current due to the following reasons: it is known that  $\text{CO}_{\text{ads}}$  cannot be formed from formic acid on isolated Pt atoms, because at least two adjacent Pt atoms are required to dehydrate formic acid molecule and form  $\text{CO}_{\text{ads}}$ , a phenomenon known as the “ensemble effect” [53]. As a result such isolated Pt atoms can be much more active towards formic acid oxidation directly to  $\text{CO}_2$ , and low Pt concentration Pd-Pt nanoalloys favor formation of such sites (a so called “third body effect” [54–56]).

Third body effect was demonstrated to be partially responsible for the volcano-type relation between formic acid oxidation peak current density and Pd concentration observed for carbon-supported Pd-Pt nanoalloys (see Fig. 4 in [17]). However here we observed the monotonic decrease of the catalytic current density as a function of composition (Fig. 5), and the difference between the mentioned literature data and our results is most probably caused by Pt surface segregation. In particular for carbon-supported Pd-Pt nanoparticles it was determined that the maximum current density is observed for nanoparticles containing ca. 10 at.% of Pt [17]. It seems probable that due to Pt surface segregation for unsupported Pd-Pt nanoparticles investigated here, the surface of our nanoparticles contains more than 10 at.% and we observe only the decreasing part of volcano-type behavior.

Discussing the density of catalytic currents in the cathodic scans (Fig. 2B) it should be mentioned that those currents can be attributed to oxidation of formic acid on freshly reduced Pd surface, as Pt or Pd surface oxides are inactive in formic acid oxidation [2]. The inactivity of Pt and Pd surface oxides towards formic acid oxidation can be confirmed by correlation between potential of formic acid oxidation in the cathodic scans (Fig. 2B) and potential of surface peak reduction (Fig. 1). In particular, the surface peak potential changed from 760 mV for pure Pd to 800 mV for pure Pt (Fig. 1). This corresponds well to onset of formic acid oxidation in the cathodic scan (Fig. 2B), which changed from 800 mV for pure Pd to 950 mV for pure Pt (Fig. 2B), taking into account that for surface oxides reduction the onset potential is ca. 150 mV higher than peak potential (Fig. 1). Together with the inactivity of Pd-Pt nanoparticle surface at high potentials where surface is covered with surface oxides (Figs. 1 and 2) it confirms a total inactivity of oxidized Pt and Pd surface towards formic acid oxidation in the investigated potential region.

It can be observed that even for nanoparticles where catalytic activity towards formic acid was already very low in the anodic scan, such as those containing 5 at.% (Fig. 3) and 10 at.% (Fig. 4) the formic acid oxidation current density in the cathodic scan was significantly larger than formic acid current density in the anodic scan (Figs. 3–5) and in general it was even larger than formic acid oxidation current density observed for pure Pd (Fig. 2B). This is illustrated in Fig. 5, where relative formic acid peak current density in the cathodic scan to the formic acid peak current density in the anodic scan was plotted as a function of Pt concentration.

To explain the observed increase of current density in the cathodic scan the conditions required for high surface activity should be discussed. In particular the prerequisites of high surface activity in the cathodic scan are the absence of both: surface

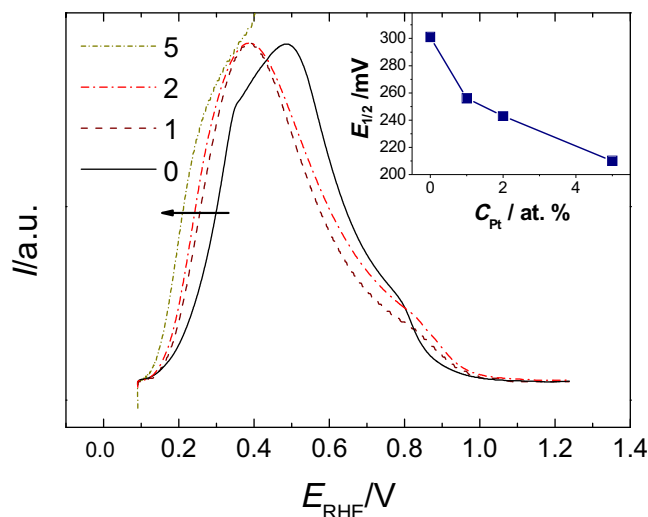


Fig. 6. Current normalized to first peak of formic acid oxidation; decrease in oxidation potential correlated to increase in Pt amount can be observed. Numbers in the legend denote Pt content in atomic percents. Inset: half-wave potential as a function of Pt content.

oxides and adsorbed carbon monoxide, which are fulfilled when potential is cycled towards more negative values, starting from at least the potential of CO oxidation (just below 1 V, see Fig. 4), and reach more negative values than potential of surface oxides reduction (at potentials from 800 mV for pure Pd to 950 mV for pure Pt (Fig. 2B)). Such conditions warrant that the surface will be reduced and CO-free, thus in state beneficial for formic acid oxidation. Adsorbed CO can be formed at relatively low potentials, thus in the cathodic scan, just after surface reduction, it is not present yet. On the contrary, in the anodic scan the bimetallic surface is already covered by adsorbed CO, which leads to decrease of its catalytic activity. Due to those facts the cathodic scans seems more indicative of the intrinsic surface catalytic activity than the anodic scans, due to possible modification of Pd surface electronic properties by presence of Pt, which exhibits as increased activity towards formic acid oxidation of Pd-Pt nanoparticles as compared to pure Pd nanoparticles. It has been also suggested that the increased current density in cathodic scan, as compared to anodic scan, is caused by the ensemble effect, but overall the changes in electronic properties also were identified as a significant factor potentially influencing the catalytic activity [17]. Both factors may play a significant role, and the role of the electronic factors will be discussed in more details during discussion of changes of formic acid half-wave potential below.

Concluding this part of the discussion, it seems that addition of Pt to Pd leads to multitude of effects, such as changes in distribution of active surface sites, introduction of separate Pt atoms and possible changes of surface electronic properties, which are together responsible for the increased catalytic activity, which for unsupported Pd-Pt nanoparticles can only be observed in the conditions where no adsorbed CO is present on the surface (such as the cathodic scan in voltammetric experiments). In certain conditions such as more effectively intermixed Pt and Pd atoms increased surface activity can be also observed in anodic scans [17]. The increase in catalytic activity for Pd-Pt nanoparticles is most probably caused by interplay between changes in electronic properties and changes in surface composition, resulting from Pt presence in Pd-Pt alloys.

To better analyze the influence of the possible changes in electronic properties for Pd-Pt nanoparticles on the catalytic activity we normalized the anodic currents in the anodic scan (as seen in Fig. 2A) to the maximum of the first anodic peak for nanoparticles containing not more than 5 at.% of Pt and we determined formic acid oxidation half-wave potential (Fig. 6).

It can be observed that the onset potential and half-wave potential of Pd-Pt nanoparticles decreased as Pt amount increased (Fig. 6). In particular half-wave potential of formic acid oxidation decreased from 300 mV for pure Pd to 210 mV for Pd-Pt containing 5 at.% of Pt. At the same time the current density decreased from  $8 \text{ mA cm}^{-2}$  to  $1 \text{ mA cm}^{-2}$  (Fig. 5).

As discussed above, the changes in surface morphology can to a large extent explain the changes in catalytic currents, and the only observation tentatively suggesting the changes in electronic properties are the difference between Pd and Pd-Pt nanoalloys catalytic activity observed in the cathodic scan. However the changes in formic acid oxidation potential (Fig. 6) cannot be fully explained by surface morphology. As a result we explain the changes in formic acid oxidation potential based on changes in the electronic properties of the Pd-Pt surface due to interactions between Pt and Pd.

There is no doubt that electronic properties play an important role in determining the catalytic activity of a given surface. Norskov and co-workers have correlated the d-band center of gravity of the catalyst (transition metal) to the adsorption energy, activation energy and dissociation energy of small molecules [57–59], and in numerous reports this correlation was confirmed (i.e. [10,60,61]). However it is unclear if the straightforward correlation between formic acid oxidation potential and calculated d-band center exists. To support this thesis it should be pointed out that despite the general agreement that the overpotential of formic acid oxidation on Pd-Pt systems (both alloys: this work and Refs. [17,18] and thin Pd layers on Pt: Refs. [10,11]) is lower than on pure Pd, however at the same time d-band center calculations show that d-band center should shift in opposite directions for those both cases:  $-0.17 \text{ eV}$  for Pd-Pt alloys and  $+0.02 \text{ eV}$  for Pd overlayer on Pt [54,58]. Concluding it seems impossible to correlate formic acid oxidation potential exclusively to the calculated d-band center energy.

It is also worth to note that increase in d-DOS close to Fermi level was observed experimentally for Pd-Pt core-shell nanoparticles and correlated to lowered formic acid oxidation potential, but at the same time experimentally determined d-band center change was negative [11]. Despite the good correlation between calculated and experimentally determined d-band center obtained for pure Pt and Pd nanoparticles, a significant discrepancy for core-shell system was observed [11]. It was then concluded that experimentally determined d-band center may behave in a more complicated way than predicted by theory for Pd monolayer over Pt nanoparticles, and actually an increase in electron density close to Fermi level (roughly equivalent in consequences to the increase of d-band center energy) may be responsible for decrease in formic acid oxidation potential due to increase in adsorption strength [11]. This points out that d-band center change is not always a good predictor of adsorption strength, and the d-DOS close to Fermi level, which is involved in adsorption process (especially  $t_{2g}$  states, located close to Fermi level [62,63]) is a better predictor of adsorption strength. Thus it cannot be excluded that a similar change of electronic properties can be expected for Pd-Pt alloys and Pd overlayers on Pt [11] as in both cases a very similar change of formic acid oxidation potential was observed, and increase in electron density close to Fermi level may be responsible for the change of the formic acid adsorption strength (seen here as increase in catalytic currents in cathodic scans for Pd-Pt as compared to pure Pd), increase in catalytic currents and decrease the formic acid oxidation potential for Pd-Pt nanoalloys. This aspect, as still unclear, is under investigation in our laboratory.

#### 4. Conclusions

We investigated the electrocatalytic activity of unsupported Pd-Pt nanoparticles with low Pt content towards formic acid oxidation.

We determined that the small addition of Pt caused significant changes in the catalytic activity observed as monotonic decrease of catalytic currents in the anodic scans of cyclic voltammograms and increase of catalytic currents in the cathodic scan by up to 80% for Pd-Pt nanoparticles as compared to pure Pd. We also observed changes in the potential of formic acid oxidation, which was 90 mV lower for Pd-Pt nanoparticles containing 5 at.% Pt, than for pure Pd nanoparticles. We attributed changes in the catalytic currents to interplay between the changes in surface composition and changes in the electronic properties of the Pd-Pt nanoparticles, where changes of half-wave potential were attributed mostly to changes in the electronic properties.

#### Acknowledgements

This project was funded from Polish National Science Centre budget based on decision number DEC-2013/09/B/ST4/00099. The study was in part carried out at the Biological and Chemical Research Centre, University of Warsaw, established within the project co-financed by European Union from the European Regional Development Fund under the Operational Programme Innovative Economy, 2007–2013. Authors would like to thank Olga Łabędź and Anna Łuciuk for collecting the TEM images and ICPMS analysis, respectively. The TEM images were obtained using the equipment purchased within CePT Project No.: POIG.02.02.00-14-024/08-00.

#### Appendix A. Supplementary data

Supplementary data associated with this article can be found, in the online version, at <http://dx.doi.org/10.1016/j.apcatb.2016.03.073>.

#### References

- [1] A. Capon, R. Parsons, Oxidation of formic-acid at noble-metal electrodes. 1. Review of previous work, *J. Electroanal. Chem.* 44 (1973) 1–7.
- [2] A. Capon, R. Parsons, Oxidation of formic-acid on noble-metal electrodes. 2. Comparison of behavior of pure electrodes, *J. Electroanal. Chem.* 44 (1973) 239–254.
- [3] A. Capon, R. Parsons, Oxidation of formic-acid at noble-metal electrodes part. 3. Intermediates and mechanism on platinum-electrodes, *J. Electroanal. Chem.* 45 (1973) 205–231.
- [4] A. Wieckowski, J. Sobkowski, A. Jablonska, Adsorption and oxidation of formic-acid on platinized electrode—test of validity of radiometric method, *J. Electroanal. Chem.* 55 (1974) 383–389.
- [5] A. Wieckowski, J. Sobkowski, Comparative study of adsorption and oxidation of formic-acid and methanol on platinized electrodes in acidic solution, *J. Electroanal. Chem.* 63 (1975) 365–377.
- [6] R. Parsons, T. Vandernoot, The oxidation of small organic-molecules—a survey of recent fuel-cell related research, *J. Electroanal. Chem.* 257 (1988) 9–45.
- [7] C. Rice, S. Ha, R.I. Masel, A. Wieckowski, Catalysts for direct formic acid fuel cells, *J. Power Sources* 115 (2003) 229–235.
- [8] X.W. Yu, P.G. Pickup, Recent advances in direct formic acid fuel cells (DFAFC), *J. Power Sources* 182 (2008) 124–132.
- [9] K. Jiang, H.X. Zhang, S.Z. Zou, W.B. Cai, Electrocatalysis of formic acid on palladium and platinum surfaces: from fundamental mechanisms to fuel cell applications, *Phys. Chem. Chem. Phys.* 16 (2014) 20360–20376.
- [10] L.A. Kibler, A.M. El-Aziz, R. Hoyer, D.M. Kolb, Tuning reaction rates by lateral strain in a palladium monolayer, *Angew. Chem. Int. Ed.* 44 (2005) 2080–2084.
- [11] M.T. Gorzkowski, A. Lewera, Probing the limits of d-band center theory: electronic and electrocatalytic properties of Pd-shell-Pt-core nanoparticles, *J. Phys. Chem. C* 119 (2015) 18389–18395.
- [12] W.P. Zhou, A. Lewera, R. Larsen, R.I. Masel, P.S. Bagus, A. Wieckowski, Size effects in electronic and catalytic properties of unsupported palladium nanoparticles in electrooxidation of formic acid, *J. Phys. Chem. B* 110 (2006) 13393–13398.
- [13] S.G. Sun, J. Clavilier, A. Bewick, The mechanism of electrocatalytic oxidation of formic-acid on Pt (100) and Pt (111) in sulfuric-acid solution—an Emirs Study, *J. Electroanal. Chem.* 240 (1988) 147–159.
- [14] M. Arenz, V. Stamenkovic, T.J. Schmidt, K. Wandelt, P.N. Ross, N.M. Markovic, The electro-oxidation of formic acid on Pt–Pd single crystal bimetallic surfaces, *Phys. Chem. Chem. Phys.* 5 (2003) 4242–4251.
- [15] H.X. Zhang, S.H. Wang, K. Jiang, T. Andre, W.B. Cai, In situ spectroscopic investigation of CO accumulation and poisoning on Pd black surfaces in concentrated HCOOH, *J. Power Sources* 199 (2012) 165–169.

- [16] J.Y. Wang, H.X. Zhang, K. Jiang, W.B. Cai, From HCOOH to CO at Pd electrodes: a surface-enhanced infrared spectroscopy study, *J. Am. Chem. Soc.* 133 (2011) 14876–14879.
- [17] H.X. Zhang, C. Wang, J.Y. Wang, J.J. Zhai, W.B. Cai, Carbon-supported Pd–Pt nanoalloy with low Pt content and superior catalysis for formic acid electro-oxidation, *J. Phys. Chem. C* 114 (2010) 6446–6451.
- [18] C. Wang, B. Peng, H.N. Xie, H.X. Zhang, F.F. Shi, W.B. Cai, Facile fabrication of Pt, Pd and Pt–Pd alloy films on Si with tunable infrared internal reflection absorption and synergetic electrocatalysis, *J. Phys. Chem. C* 113 (2009) 13841–13846.
- [19] X. Li, I.M. Hsing, Electrooxidation of formic acid on carbon supported  $Pt_xPd_{1-x}$  ( $x=0-1$ ) nanocatalysts, *Electrochim. Acta* 51 (2006) 3477–3483.
- [20] J.A. Rodriguez, R.A. Campbell, D.W. Goodman, Electronic interactions in bimetallic systems—an X-ray photoelectron spectroscopic study, *J. Phys. Chem.* 94 (1990) 6936–6939.
- [21] J.A. Rodriguez, R.A. Campbell, D.W. Goodman, Electronic interactions in bimetallic systems—core-level binding-energy shifts, *J. Vac. Sci. Technol. A* 9 (1991) 1698–1702.
- [22] J.A. Rodriguez, D.W. Goodman, The nature of the metal bond in bimetallic surfaces, *Science* 257 (1992) 897–903.
- [23] R.A. Campbell, J.A. Rodriguez, D.W. Goodman, V. Ponc, D.A. King, H. Niemantsverdriet, R. Vansanten, W. Grunert, D. Chadwick, J.C. Bertolini, D. Wang, Nature of metal–metal bonding in mixed-metal catalysts, *Stud. Surf. Sci. Catal.* 75 (1993) 333–344.
- [24] A. Lewera, W.P. Zhou, R. Hunger, W. Jaegermann, A. Wieckowski, S. Yockel, P.S. Bagus, Core-level binding energy shifts in Pt–Ru nanoparticles: a puzzle resolved, *Chem. Phys. Lett.* 447 (2007) 39–43.
- [25] M.A. Rigsby, W.P. Zhou, A. Lewera, H.T. Duong, P.S. Bagus, W. Jaegermann, R. Hunger, A. Wieckowski, Experiment and theory of fuel cell catalysis: methanol and formic acid decomposition on nanoparticle Pt/Ru, *J. Phys. Chem. C* 112 (2008) 15595–15601.
- [26] P. Serp, B. Machado, Nanostructured Carbon Materials for Catalysis, Royal Society of Chemistry, 2015.
- [27] C.A. Bessel, K. Laubernds, N.M. Rodriguez, R.T.K. Baker, Graphite nanofibers as an electrode for fuel cell applications, *J. Phys. Chem. B* 105 (2001) 1115–1118.
- [28] I.S. Park, K.W. Park, J.H. Choi, C.R. Park, Y.E. Sung, Electrocatalytic enhancement of methanol oxidation by graphite nanofibers with a high loading of PtRu alloy nanoparticles, *Carbon* 45 (2007) 28–33.
- [29] F. Rodriguez-Reinoso, The role of carbon materials in heterogeneous catalysis, *Carbon* 36 (1998) 159–175.
- [30] J.W. Ma, A. Habrioux, C. Morais, A. Lewera, W. Vogel, Y. Verde-Gomez, G. Ramos-Sanchez, P.B. Balbuena, N. Alonso-Vante, Spectroelectrochemical probing of the strong interaction between platinum nanoparticles and graphitic domains of carbon, *ACS Catal.* 3 (2013) 1940–1950.
- [31] J.W. Ma, A. Habrioux, M. Pisarek, A. Lewera, N. Alonso-Vante, Induced electronic modification of Pt nanoparticles deposited onto graphitic domains of carbon materials by UV irradiation, *Electrochem. Commun.* 29 (2013) 12–16.
- [32] S.C. Fung, S.J. Tauster, R.T.K. Baker, J.A. Horsley, R.L. Garten, Properties of metal-catalysts altered by strongly interacting oxide supports, *Am. Chem. Soc.* 179 (1980) 94–Coll, Abstract Paper.
- [33] S.C. Fung, S.J. Tauster, R.T.K. Baker, R.L. Garten, Strong metal-support interactions—group-VIII noble-metals supported on transition-metal oxides, *Am. Chem. Soc.* (1979) 174, Abstract Paper.
- [34] S.J. Tauster, S.C. Fung, R.L. Garten, R.T.K. Baker, J.A. Horsley, Strong interactions at metal-oxide interfaces, *Am. Chem. Soc.* (1979) 167, Abstract Paper.
- [35] S.J. Tauster, S.C. Fung, R.L. Garten, Strong metal-support interactions—group-8 noble-metals supported on  $TiO_2$ , *J. Am. Chem. Soc.* 100 (1978) 170–175.
- [36] S. Blair, D. Lycke, C. Iordache, Palladium–platinum alloy anode catalysts for direct formic acid fuels, *ECS Trans.* (2006) 1325–1332.
- [37] M.S. McGovern, E.C. Garnett, C. Rice, R.I. Masel, A. Wieckowski, Effects of Nafion as a binding agent for unsupported nanoparticle catalysts, *J. Power Sources* 115 (2003) 35–39.
- [38] P. Waszczuk, T.M. Barnard, C. Rice, R.I. Masel, A. Wieckowski, A nanoparticle catalyst with superior activity for electrooxidation of formic acid, *Electrochem. Commun.* 4 (2002) 599–603.
- [39] A. Januszewska, G. Dercz, J. Piwowar, R. Jurczakowski, A. Lewera, Outstanding catalytic activity of ultra-pure platinum nanoparticles, *Chem. Eur. J.* 19 (2013) 17159–17164.
- [40] A. Lewera, W.P. Zhou, C. Vericat, J.H. Chung, R. Haasch, A. Wieckowski, P.S. Bagus, XPS and reactivity study of bimetallic nanoparticles containing Ru and Pt supported on a gold disk, *Electrochim. Acta* 51 (2006) 3950–3956.
- [41] A. Januszewska, G. Dercz, A. Lewera, R. Jurczakowski, Spontaneous chemical ordering in bimetallic nanoparticles, *J. Phys. Chem. C* 119 (2015) 19817–19825.
- [42] C. Michaelsen, On the structure and homogeneity of solid-solutions—the limits of conventional X-ray-diffraction, *Philos. Mag. A* 72 (1995) 813–828.
- [43] M.W. Breiter, Adsorption and oxidation of carbon-monoxide on smooth palladium in sulfuric-acid-solution, *J. Electroanal. Chem.* 109 (1980) 243–251.
- [44] K. Kunitatsu, Adsorption of carbon-monoxide on a smooth palladium electrode—an Insitu Infrared Spectroscopic Study, *J. Phys. Chem.* 88 (1984) 2195–2200.
- [45] B. Losiewicz, L. Birry, A. Lasia, Effect of adsorbed carbon monoxide on the kinetics of hydrogen electrosorption into palladium, *J. Electroanal. Chem.* 611 (2007) 26–34.
- [46] D.A.J. Rand, R. Woods, Nature of adsorbed oxygen on rhodium, palladium and gold electrodes, *J. Electroanal. Chem.* 31 (1971) 29.
- [47] M. Baldauf, D.M. Kolb, Formic acid oxidation on ultrathin Pd films on Au(hkl) and Pt(hkl) electrodes, *J. Phys. Chem.* 100 (1996) 11375–11381.
- [48] G.Q. Lu, A. Crown, A. Wieckowski, Formic acid decomposition on polycrystalline platinum and palladized platinum electrodes, *J. Phys. Chem. B* 103 (1999) 9700–9711.
- [49] K. Brandt, M. Steinhausen, K. Wandelt, Catalytic and electro-catalytic oxidation of formic acid on the pure and Cu-modified Pd(111)-surface, *J. Electroanal. Chem.* 616 (2008) 27–37.
- [50] S. Pronkin, M. Hara, T. Wandlowski, Electrocatalytic properties of Au(111)-Pd quasi-single-crystal film electrodes as probed by ATR-SEIRAS, *Russ. J. Electrochem.* 42 (2006) 1177–1192.
- [51] H. Miyake, T. Okada, G. Samjeske, M. Osawa, Formic acid electrooxidation on Pd in acidic solutions studied by surface-enhanced infrared absorption spectroscopy, *Phys. Chem. Chem. Phys.* 10 (2008) 3662–3669.
- [52] M.R. Columbia, P.A. Thiel, The interaction of formic-acid with transition-metal surfaces, studied in ultrahigh-vacuum, *J. Electroanal. Chem.* 369 (1994) 1–14.
- [53] S. Park, Y. Xie, M.J. Weaver, Electrocatalytic pathways on carbon-supported platinum nanoparticles: comparison of particle-size-dependent rates of methanol, formic acid, and formaldehyde electrooxidation, *Langmuir* 18 (2002) 5792–5798.
- [54] U.B. Demirci, Theoretical means for searching bimetallic alloys as anode electrocatalysts for direct liquid-feed fuel cells, *J. Power Sources* 173 (2007) 11–18.
- [55] M. Watanabe, M. Horiuchi, S. Motoo, Electrocatalysis by Ad-atoms. 23. Design of platinum Ad-electrodes for formic-acid fuel-cells with Ad-atoms of the 4th-group and the 5th-group, *J. Electroanal. Chem.* 250 (1988) 117–125.
- [56] E. Leiva, T. Iwasita, E. Herrero, J.M. Feliu, Effect of adatoms in the electrocatalysis of HCOOH oxidation. A theoretical model, *Langmuir* 13 (1997) 6287–6293.
- [57] B. Hammer, Y. Morikawa, J.K. Nørskov, CO chemisorption at metal surfaces and overlayers, *Phys. Rev. Lett.* 76 (1996) 2141–2144.
- [58] A. Ruban, B. Hammer, P. Stoltze, H.L. Skriver, J.K. Nørskov, Surface electronic structure and reactivity of transition and noble metals, *J. Mol. Catal. A: Chem.* 115 (1997) 421–429.
- [59] E. Christoffersen, P. Liu, A. Ruban, H.L. Skriver, J.K. Nørskov, Anode materials for low-temperature fuel cells: a density functional theory study, *J. Catal.* 199 (2001) 123–131.
- [60] S. Alayoglu, A.U. Nilekar, M. Mavrikakis, B. Eichhorn, Ru–Pt core-shell nanoparticles for preferential oxidation of carbon monoxide in hydrogen, *Nat. Mater.* 7 (2008) 333–338.
- [61] A.U. Nilekar, S. Alayoglu, B. Eichhorn, M. Mavrikakis, Preferential CO oxidation in hydrogen: reactivity of core-shell nanoparticles, *J. Am. Chem. Soc.* 132 (2010) 7418–7428.
- [62] T. Hofmann, T.H. Yu, M. Folse, L. Weinhardt, M. Bar, Y.F. Zhang, B.V. Merinov, D.J. Myers, W.A. Goddard, C. Heske, Using photoelectron spectroscopy and quantum mechanics to determine d-band energies of metals for catalytic applications, *J. Phys. Chem. C* 116 (2012) 24016–24026.
- [63] M.P. Hyman, J.W. Medlin, Effects of electronic structure modifications on the adsorption of oxygen reduction reaction intermediates on model Pt(111)-alloy surfaces, *J. Phys. Chem. C* 111 (2007) 17052–17060.